# HIGH SPEED PLASMA STREAMS IN VACUUM ARCS

A. A. PLYUTTO, V. N. RYZHKOV, and A. T. KAPIN

Submitted to JETP editor October 3, 1963

J. Exptl. Theoret. Phys. (U.S.S.R.) 47, 494-507 (August, 1964)

Results of investigation of high speed plasma streams in stationary vacuum arcs are presented. The mean energies of the ions of metals of the first group (Mg, Al, Ni, Cu, Ag) are 20—40 eV. The presence of significant quantities of doubly and triply charged ions of metals of the second group in the plasma is established spectroscopically. The concept of a potential hump in the cathode spot region is introduced to explain the origin of the high speed plasma streams.

## 1. INTRODUCTION

HIGH speed plasma streams that emerge from the cathode region of vacuum arcs have been investigated since 1930, when Tanberg[1] observed this unusual physical phenomenon. For arcs with copper cathodes, the average particle energies measured by Tanberg reached 80 eV, corresponding to a temperature of $5 \times 10^5$ deg K in the cathode region. However, his pyrometric and spectroscopic estimates[2] have shown that the temperature does not exceed $3 \times 10^3$ deg K. High speed plasma streams were observed also in arcs from Hg[3,4], Al, Fe, Mg, Zn, Au, Ag, Cd, Mo, and Sn[5]. It was established in these investigations that the plasma streams exert anomalously large reaction forces on the cathodes. Robertson[6] found that the forces increase from 2.5 to 15 dyne/A as the pressure of the gas $(N_2)$ decreases from 6 to 0.3 mm Hg respectively.

Compton[7] proposed that the reaction forces are due to recombination and reflection of a fraction of the ions accelerated by the cathode potential drop from the cathode surface. However, such a mechanism cannot explain the dependence of the forces on the gas pressure. Tonks has shown[8] that the pressure of the electron gas in the cathode spots can result in reaction forces close to those observed in experiment. He did not consider, however, the forces that keep the extremely light electron cloud at the surface of the cathode, or the causes of the high velocity plasma streams. Other attempts at explaining the experimental facts are quite far-fetched and cannot withstand a careful scrutiny.

After 1938 the focus of the vacuum-arc physics research shifted to the study of the spot-to-spot motion[9,10], stability,[6,11,12], determination of the current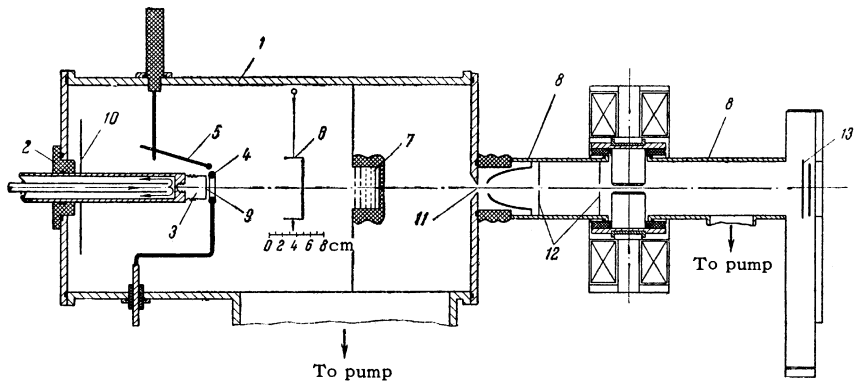 density at the cathode spots[13-15], and others. Several models were proposed for the near-cathode region, and appreciable progress was made towards explaining the mechanism of electron emission in the cathode spots[16]. However, the singularities of vacuum arcs and in particular the causes of high velocity plasma streams could not be explained from a single point of view.

The authors of the present article have proposed previously[17] a mechanism for ambipolar acceleration of ions by electrons. This mechanism made it possible to explain also the appearance of high velocity plasma streams in stationary vacuum arcs. However, since the available experimental data were insufficient and contradictory, the need for additional experiments arose. We present below the results of more accurate investigations of high-velocity plasma streams and propose a cathode-region model that explains many of the experimental facts.

## 2. EXPERIMENTAL SETUP

The experiments were made with the setup drawn to scale in Fig. 1. The steel working chamber 1 had a volume of 50 liters. A cooled holder with cathode 3 was inserted through a side flange and insulator 2. The anode 4 was secured to an uncooled electrode holder. Tungsten rod 5 was used to ignite the arc by contact. The pendulum 6, the analyzer probe 7, and the mass-spectroscopic analyzer 8 were located behind the anode (the cathode and anode could be moved along the chamber axis). The working chamber had two viewing windows for observation of the arc and of the deflection of the pendulum. The high-vacuum system comprised a diffusion pump with a capacity of 1,000 liters per second. The arc was fed from a dc machine (350 A, 150 V). The arc current was regulated with an electrolytic rheostat. The working

FIG. 1. Diagram of experimental setup.

chamber was not grounded and was under a float-
ing potential relative to the arc plasma.

## 3. EXPERIMENTS ON THE STABILIZATION OF VACUUM ARCS

The very first experiments on the ignition of
vacuum arcs with currents up to 50 A have shown
that at pressures above $10^{-1}$—$5 \times 10^{-2}$ mm Hg the
arc burns stably and is sufficiently steady when
different metals are used. At lower pressures
(to $10^{-3}$–$10^{-5}$ mm Hg) the arc becomes unstable
and is extinguished within a fraction of a second.
Under these conditions the arc is also unsteady
(the cathode spots move off the working surface
of the cathode 9, see Fig. 1). Searches for stable
and steady arc combustion modes over a time nec-
essary for the performance of the experiments
(2—10 seconds) were made by varying the shape
and material of the cathode, the shape of the anode
and its placement relative to the cathode, the loca-
tion of the electrode holders and their material,
by screening the junctions between the holders and
the insulator, etc.

Stable and steady arc combustion became feas-
ible at currents up to 50 amperes with cathodes
made of zinc, cadmium, magnesium, bismuth, and
lead, which are characterized by a low boiling
temperature (770—1750°K). Arcs from copper,
nickel, silver, aluminum, and beryllium, metals
with a high boiling temperature (2200—3000°K),
are unsteady under such conditions. A steady arc
can be produced by alloying copper with zinc (the
content of the latter being from 5 to 20%), and also
by using brass (LS-59). It can be assumed that
stable and steady vacuum arcs can be produced
also with other alloys of metals from groups I and
II.

Stabilization of the arc by increasing the current
to 250 A was observed for all metals with the ex-
ception of Be, Ta, W, and Mo. Thus, for Ag, Ni,
and Cu the arc burns stably and steadily even at

currents of 100—120 A.

To prevent the cathode spots from moving off
the working surface 9, grooves were cut on the
side surface of the cathode, or else composite
cathodes were used. The investigated metal was
pressed into the cavity of a bulky steel frame or
was placed in a tantalum cylinder. The shape of
the anode exerts no noticeable influence on the
combustion of the arc if the anode is placed 5—15
mm in front of the working surface of the cathode.
(Coaxial placement of an annular anode in the
plane of the working surface of the cathode makes
the arc unstable.)

The optimal geometry and relative placement of
the electrodes were found (Fig. 1) after numerous
experiments on the stabilization of vacuum arcs.
The cathode holder electrode was made of stain-
less steel. To prevent an arc from being formed
on the junction with the insulator 2, the latter was
screened by a metallic disc 10. The toroidal (ring)
anode was made of tantalum wire and had symmet-
rical current leads. The anode was not forced-
cooled and its energy was dissipated essentially by
radiation. The use of an anode having a diameter
somewhat larger than the cathode made it possible
to eliminate almost completely the distortion due
to the shadow cone of the anode and to secondary
evaporation of the metal from its surface.

## 4. GENERAL CHARACTER OF EVAPORATION OF THE CATHODE MATERIAL AND ANGULAR DISTRIBUTION

The experiments on vacuum arc stabilization
showed that during the arc combustion the cathode
material is consumed both in the form of a plasma
stream and in the form of individual macroparti-
cles. The spatial distributions of the plasma
streams and of the macroparticles are essentially
different. The maximum plasma densities are ob-
served along the axis of the system, and the maxi-
mum flux of macroparticles is in the plane of the

working surface of the cathode and is confined to small angles. The relative amount of macroparticles depends to a considerable degree on the cathode material, on the combustion time, and on the arc current. In particular, when working with cathodes made of brass (LS-59) and magnesium, there are practically no macroparticles at currents up to 100 A and at combustion times not exceeding 5 seconds. Under the same conditions, when working with cathodes made of aluminum, silver, and copper, the number of macroparticles reaches 60–80% of the total amount of matter. The angular distribution of the macroparticles was not investigated in detail, although it can be stated that practically no macroparticles enter the solid angle 60–70° (on the axis of the system), if the arc is ignited from the working surface of the cathode.

The plasma streams flowing at considerable distances from the cathode are linear and follow the radii of a hemisphere. The velocity of directional motion is somewhat higher than thermal velocity, this being confirmed by the existence of sharp shadows on any obstacle placed in the path of the plasma stream. To investigate the angular distribution of the plasma streams, experiments were made, in which a set of 9 plates was arranged in a circle behind the anode, 8 cm from the center of the working surface of the cathode. The character of the angular distribution of the masses was determined by weighing the plates. To eliminate errors due to the macroparticles, the experiments were made with a brass cathode, at an arc current of 100 A and a duration of 5 seconds for each exposure. The plasma stream angular distribution obtained in this manner is in good agreement with the cosine law.

In control experiments the amount of sputtered material (plasma) was determined both by weighing the cathode and by integrating the current density with allowance for the cosine law. In this case the discrepancy did not amount to 15–20%, probably because of the reflection of the particles from the condensation plates. Special experiments have shown that the coefficient of accommodation actually reaches 85–80% under these conditions. This integration method was therefore used in all further experiments to determine the amount of evaporated substance.

## 5. MEASUREMENT OF THE AVERAGE VELOCITY OF PLASMA STREAMS BY THE PENDULUM METHOD

The pendulum measurement method was used in many investigations [1,5,6,18] either to determine the velocity of the plasma streams or to estimate the reaction forces on the cathode. However, owing to the difficulty in maintaining a stable and steady arc combustion in vacuum, these measurements cannot be regarded as sufficiently reliable. For example, Tanberg[1] used a cathode with a quartz mount to facilitate the combustion of the arc at the junction between the copper and the quartz, so that the measured velocities turn out to be appreciably overestimated (owing to the evaporation of the quartz).

Easton, Lucas, and Creedy[5] investigated essentially pulsed arcs, but did not account for the influence of the transients. The measurements of Robertson[6] were made at gas pressures not lower than $10^{-1}$ mm Hg. It has therefore become necessary to carry out experiments under cleaner conditions.

In most measurements of the average plasma stream velocity in stationary vacuum arcs, we used a pendulum 9 cm in diameter and 4 cm deep, located 10 cm away from the cathode. Such an experimental geometry has made it possible to compare our results with those obtained previously[1,5]. The average value of the normal velocity component was determined from the deflecting force and the increase in pendulum mass per unit time. The true velocity was determined by introducing corrections for the angular distribution of the mass and for the accommodation coefficient. However, since these corrections were approximately of the same order of magnitude and of opposite signs, the measured values of the velocities turned out to be quite close to the true values.

It must be noted that pendulum measurements were made with short-duration arcs (3–5 seconds) and the cathode temperature did not have a chance to assume a stationary value, so that the deflection of the pendulum increased during the course of the experiment by 20–25%, owing to the increased evaporation of matter from the cathode.

The angular distribution of the velocities was obtained with the aid of a cylindrical pendulum of small diameter (3 cm). The measurements were made with a brass cathode. The pendulum was mounted at angles zero, 22.5, 45, and 60° to the system axis. These experiments showed that the plasma velocities (within the limits of a ±10% experimental accuracy) do not depend on the direction of motion and on the average amount to 8.5 × $10^5$ cm/sec for brass.

The measured plasma velocities for different metals, and other characteristics of vacuum arcs, are listed in Table I.

It follows from Table I that the average veloci-

## Table I

| Cathode metal | Arc current, A | Arc voltage, V | Total consumption of material 10⁻⁵ g/C | Consumption of material in the form of plasma, 10⁻⁵ g/C | Pendulum measurements | | | Probe measurements | |
|---|---|---|---|---|---|---|---|---|---|
| | | | | | Average plasma velocity, $10^5$ cm/sec | Average plasma energy, eV | Average energy given in[5], eV | Average ion energy, eV | Average energy with allowance for charge multiplicity, eV |
| 1 | 2 | 3 | 4 | 5 | 6 | 7 | 8 | 9 | 10 |
| Mg | 50 | 13.4 | | | | | 4.0 | | |
| | 100 | 14.2 | | | | | | 15.2±0.3 | 22±2 |
| | 170 | 15.0 | 3.6 | 4.2(2.5) | 8,8(15) | 9,5(27,0) | | 18.6±0.4 | 27±3 |
| Al | 100 | 20.0 | | | | | 9.4 | | |
| | 300 | 20.8 | 12 | 6(2.3) | 6,5(17) | 5,8(40,8) | | 26.3±0.5 | 37±4 |
| Ni | 100 | 18.0 | | | | | | 25.3±0.5 | 34±4 |
| | 300 | 19.6 | 10 | 5(3,9) | 7(9) | 15(24.5) | | 21.6±0.4 | 29±3 |
| Cu | 20 | | | | | | 69.5 | | |
| | 100 | 19.2 | | | | | | 25.0±0.5 | |
| | 300 | 20.0 | 13 | 6.5(5.2) | 7.8(9.7) | 20,0(31.0) | | 23.5±0.5 | |
| Ag | 100 | 16.5 | | | | | | 25.2±0.5 | |
| | 166 | | | | | | 22.0 | | |
| | 300 | 17.8 | 14 | 7.2 | 8.4 | 39,0 | | 9.0±0.2 | |
| Zn | 20 | 11.0 | | | | | 40.0 | | |
| | 57 | | | | | | | | |
| | 100 | 12.0 | | | | | | 8.2±0.2 | |
| | 300 | 12.5 | 32 | 16(13) | 2.3(2.9) | 2.2(3.4) | | | |
| Cd | 43 | | | | | | 0,6 | | |
| | 50 | 10.5 | | | | | | 5.6±0.1 | 5.7±0.15 |
| | 100 | 10.8 | | | | | | 5.0±0.1 | 5.0±0.15 |
| | 170 | 11.1 | 62 | 31 | 1.8 | 1.9 | | | |
| Pb | 20 | 10.3 | | | | | | 9.5±0.2 | |
| LS-59 | 100 | 14.0 | 5.9 | 4.4(3.5) | 8.5(11) | 24.0(36.0) | | 20.0±0.4 | |
| | 285 | 14.5 | 8.4 | 7.8(6.3) | 6,1(7.6) | 12,0(19.0) | | | |

ties of the plasma streams do not exceed $9 \times 10^5$ cm/sec (without correction for oxidation). For metals with low boiling temperatures and poor thermal conductivities (Zn, Cd, Pb, Bi) the average velocities turned out to be quite low, and the consumption of material high. It must be noted that for these metals pendulum measurements are not sufficiently reliable. We made no measurements with mercury, but it can be stated that the velocities measured by Kobel[3] [(1.6—4) $\times 10^6$ cm/sec] are highly exaggerated. From a comparison of columns 7 and 8 of Table I it follows that the plasma velocities differ greatly for stationary and pulsed vacuum arcs.

It must be emphasized that a thin layer of the metal condensed on the pendulum is oxidized after air is admitted into the chamber. The degree of oxidation of the layer is difficult to establish, and this introduces a noticeable uncertainty in the pendulum method. The corrections (numbers in the parentheses) in Table I are based on the assumption that the oxidation of the layer is complete.

The pendulum measurements have confirmed quite clearly the existence of high velocity plasma streams in stationary vacuum arcs from different metals. However, the accuracy of the pendulum measurements is low. Furthermore, such char-

acteristics of plasma streams as the energy distribution of the particles, the degree of ionization, the electron temperature, etc. remain unexplained. To determine these characteristics, we used an electrostatic probe analyzer.

## 6. EXPERIMENTS WITH ELECTROSTATIC PROBE ANALYZER

The electrostatic probe analyzer (see Fig. 2) is intended for separation of the ionic component of the plasma with subsequent analysis based on the energy per unit charge, using the retarding potential method. The probe has 5 plane-parallel electrodes contained in a cylindrical insulator I. Each of the plates II and III had in its center 5 holes of diameter 0.5 and 1 mm, respectively. Electrodes IV and V were in the form of grids (mesh $1 \times 1$ mm, transmission coefficient 40%). Plate VI served as an ion collector. The probe was mounted on a copper panel 7. The entrance diaphragm of the probe (plate II) was in constant electric contact with the grid V and with the housing of the chamber, while electrode III was connected to grid IV.

To separate the ionic component, a potential of −100 V is applied to electrode III. The ions accelerated in the gap II—III passed through the equipo-
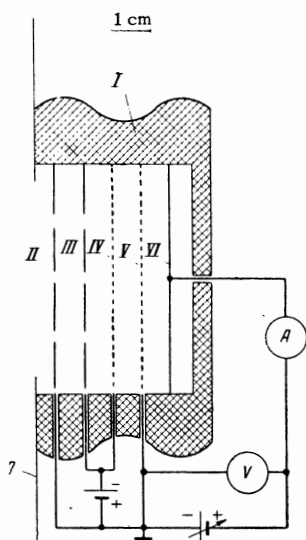
FIG. 2. Section through electrostatic probe-analyzer.

Each point of the probe voltage-current charac-
teristic was an average of 5—10 measurements.
The need for using statistics is connected with the
variation of the character of arc combustion from
ignition to ignition. When plotting each current-
voltage characteristic, several control measure-
ments were made with zero retarding potential.
The energy spectrum of the ions per unit charge
was determined by numerical differentiation of the
probe characteristics.

The ion energy distribution curves for different
metals are shown in Fig. 3. The average energies
(per unit charge) for metals of the first group (Zn,
Cd, Pb) amounts to 5—10 eV, while those of the
second group (Al, Cu, Mg, Ni, Ag) amounts to
18—25 eV (Table I). Each point of the curves of
Fig. 3 was the result of 50—70 measurements. The
accuracy reached in this case ± 1.5%. (When work-
ing with Mg, production of a MgO film can intro-
duce appreciable errors in repeated measurements
after the air is admitted into the vacuum system).

The average ion velocities are close to those
obtained with pendulum measurements (Table I,
Column 7, numbers in parentheses).

The energy spectrum of the ions is quite broad
for the second group of metals (0—70 eV), and
much narrower for the first group (0—25 eV). The
general character of the energy distribution differs
appreciably from Maxwellian. The distribution
curve shows several intense ion groups. When the
arc current is increased to 300 A, the distribution
becomes closer to Maxwellian, the average and
maximum energies of the ions become somewhat
smaller, and the distribution curve is smoothed
out.

Inasmuch as the increase in current also sta-
bilizes the arc, it can be assumed that the energy
distribution of the ions is connected with the insta-
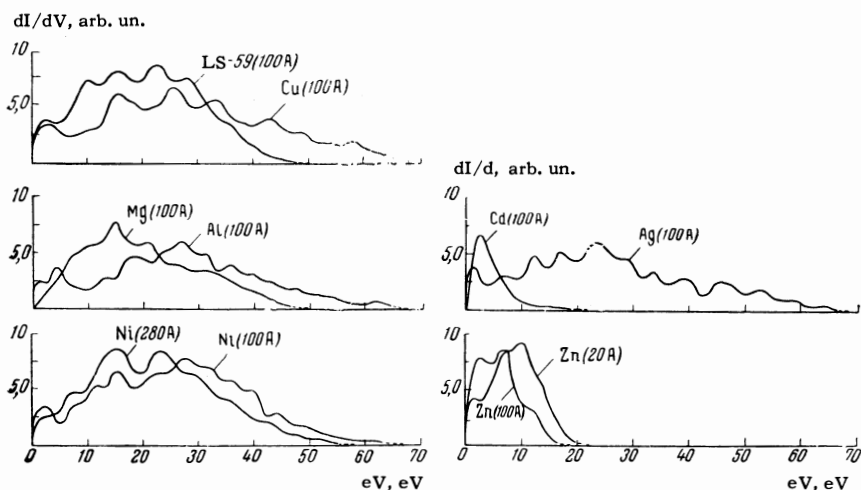bilities of the arc. External instabilities should

tential space III—IV and were slowed down to their
initial velocities between grids IV—V, proceeding
to collector VI. The retarding potential on the col-
lector was varied (in steps of 1.5 V) from −20 to
+100 V; the dc component of the ion current was
registered with a type M-193 meter. The probe
was placed in the chamber behind the anode and
20 cm from the arc (see Fig. 1).

Most experiments were made at an arc current
of 100 A. The arc was ignited at equal time inter-
vals (0.5 or 1 minute) and burned for 1.5—2 sec-
onds. This was necessary in order to maintain the
cathode temperature constant from measurement
to measurement. The ion current to the collector
reached a maximum directly after the turning on
of the arc, but then decreased gradually. The read-
ings were taken at maximum current. The decrease
of the collector current is apparently connected
with the deterioration of the vacuum within the
volume of the probe.



FIG. 3. Distribution of ions by energies
(per unit charge) for different metals (num-
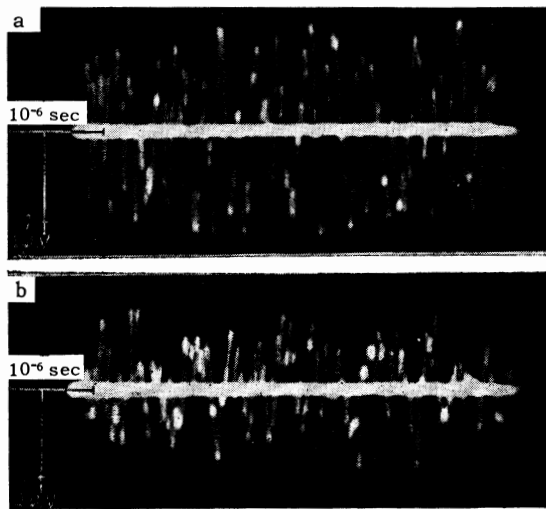ber in parentheses — arc current).

FIG. 4. Oscillograms of arc-voltage pulsations: a — arc current 100 A, b — 300 A.

be manifest in pulsations of the arc voltage and current. Random pulsations of voltage, with durations $(3-8) \times 10^{-7}$ sec and with amplitudes up to $1-1.5$ eV, were registered at arc currents $25-100$ A with all metals. An increase in the arc current to 300 A greatly reduced the amplitude of the voltage pulsations (see Fig. 4). The instabilities of the arc may be responsible for the appearance of individual groups of ions. In particular, the more energetic ions may appear when the arc voltage is higher. However, the small relative magnitude of the voltage pulsations (not more than $\pm 10\%$) can hardly explain the large energy scatter of the ions.

It must be noted that the character of the energy spectrum can depend to a considerable degree on the presence of multiply charged ions. In particular, ions which have lost (as a result of charge exchange) part of the charge after acceleration will be registered at larger retarding potentials. The average energies will obviously also depend on the relative content of ions with different charge multiplicities. The results of probe measurements may turn out to be insufficiently reliable in such a case.

A mass spectroscopic analysis of the plasma composition was made to refine the results of the probe measurements.

## 7. MASS SPECTROSCOPIC ANALYSIS OF THE PLASMA OF VACUUM ARCS

To analyze the ion composition of the plasma of vacuum arcs, a Thomson mass spectroscope was used (the method of parabolas; part 8 of Fig. 1). The analyzer was at a high potential ($-10$ kV) relative to the arc chamber. The plasma pene-

trated into the ion-gathering region through a millimeter hole 11 (the arc cathode was located 15 cm from the hole 11). The collected ion current was $200-300\,\mu$A at an arc current of 100 A. No special means were used to focus the ion beam. The beam was collimated by two 1-mm holes 12. The ion spectrum could be observed on the screen 13 and photographed.

A typical mass spectrogram obtained with a copper cathode is shown in Fig. 5. The main spectrum (ions which do not change charge in the analyzer volume) contains $Cu^{+1}$, $Cu^{+2}$, $Cu^{+3}$, and $Cu^{+4}$ (the ions $Al^{+1}$ and $Al^{+2}$ are impurities). Located below are the charge-exchanged ions: $Cu^{+3} \rightarrow Cu^{+2}$, $Cu^{+2} \rightarrow Cu^{+1}$, $Cu^{+3} \rightarrow Cu^{+1}$, $Cu^{+4} \rightarrow Cu^{+1}$, and $Al^{+2} \rightarrow Al^{+1}$. The charge-exchanged ions lie on a line passing through the zero spot and the given point of the main spectrum (stripping processes are insignificant under these conditions). The ions that have lost a charge between the poles of the magnet form strips of weak intensity. The causes of the star-like structure of the spectral points are as yet unclear.

Analogous spectra was obtained also for other metals, for which probe measurements were made. The ions registered in this case are listed in Table II. Slight amounts of $H^{+1}$, $H_2^{+1}$, $H_3^{+1}$, and $C^{+1}$ are present in all the mass spectrograms. It is interesting to note that the spectrum of stationary vacuum arcs approaches the spectrum of inductively-coupled sparks[19].

Quantitative measurements of the ion composition of the plasma were made with the aid of a system of collectors lying in the plane of the photographic plate in accordance with the position of the points of the main spectrum. One of the collectors registered the current of the charge-exchanged ions. The beams were aimed on the collectors by the deflecting fields of the analyzer. The data were
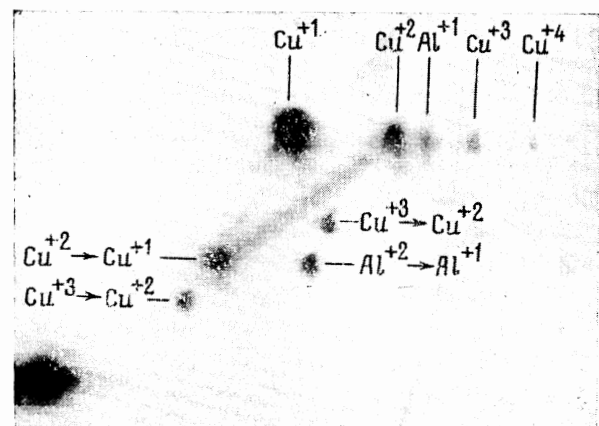


FIG. 5. Mass spectrogram for copper.

Table II

| Cathode metal | Degree of ionization, percent | Ions registered on mass spectrograms | Ion content*, % | | |
|---|---|---|---|---|---|
| | | | i=+1 | i=+2 | i=+3 |
| Mg | 80—100 | $Mg^{+1}$, $Mg^{+2}$, $Mg^{+2} \to Mg^{+1}$ | 50±5 | 50±5 | 0 |
| Al | 50—60 | $Al^{+1}$, $Al^{+2}$, $Al^{+3}$, $Al^{+3} \to Al^{+2}$, $Al^{+2} \to Al^{+1}$, $Al^{+3} \to Al^{+1}$ | 60,0±4,5 | 38±4 | 2±0,5 |
| Ni | 60—70 | $Ni^{+1}$, $Ni^{+2}$, $Ni^{+3}$, $Ni^{+3} \to Ni^{+2}$, $Ni^{+3} \to Ni^{+1}$, $Ni^{+2} \to Ni^{+1}$ | 6,5±4,5 | 33±4 | 2,0±0,5 |
| Cu | | $Cu^{+1}$, $Cu^{+2}$, $Cu^{+3}$, $Cu^{+4}$, $Cu^{+4} \to Cu^{+3}$, $Cu^{+3} \to Cu^{+1}$, $Cu^{+2} \to Cu^{+1}$, $Cu^{+3} \to Cu^{+2}$ | | | |
| Ag | 50—60 | $Ag^{+1}$, $Ag^{+2}$, $Ag^{+3}$, $Ag^{+3} \to Ag^{+2}$, $Ag^{+3} \to Ag^{+1}$, $Ag^{+2} \to Ag^{+1}$ | | | |
| Zn | 15—20 | $Zn^{+1}$, $Zn^{+2}$, $Zn^{+2} \to Zn^{+1}$ | | | |
| Cd | 12—15 | $Cd^{+1}$, $Cd^{+2}$, $Cd^{+2} \to Cd^{+1}$, | 99,7±0,05 | 0,3±0,05 | 0 |
| Pb | 18—25 | $Pb^{+1}$, $Pb^{+2}$, $Pb^{+2} \to Pb^{+1}$ | | | |
| LS-59 | 60—70 | $(Cu/Zn)^{+1}$, $(Cu/Zn)^{+2}$, $(Cu/Zn)^{+3}$, $(Cu/Zn)^{+3} \to (Cu/Zn)^{+2}$, $(Cu/Zn)^{+2} \to (Cu/Zn)^{+1}$, $(Cu/Zn)^{+3} \to (Cu/Zn)^{+1}$ | | | |

*Ion content calculated by the formula $I_i = \sum\limits_{i=1}^{3} I^i$, where $I^i$ — number of ions with charge multiplicity i.

checked against those for the singly-charged ions. The retarding potential ( − 80 V ) suppressed the secondary electron emission.

The measured percentage contents of some metals (determined from the number of particles) are listed in Table II. The charge-exchanged ions were included in the estimated percentage content of doubly charged ions. The mass spectroscopic analysis has shown that in a plasma of metals of the first group the singly-charged ions predominate completely. In the second group of metals, the doubly charged ions amount up to 50%, while in triply charged ones—up to 2%. The absence of triply changed ions in the spectrum of Mg is due to the high third ionization potential (79.4 V).

The relative content of neutral particles (degree of plasma ionization) was determined from the densities of plasma and ion flow to the metallic plate. The degree of ionization of the plasma reached 25% for metals of the first group and 50—100% for metals of the second group (see Table II). The errors connected with oxidation were not appreciable in these experiments, since the thickness of the sputtering layer was much larger than in pendulum measurements.

It must be noted that the content of multiply charged ions decreases greatly with increasing arc current. A change in the arc-chamber pressure from $5 \times 10^{-5}$ to $1 \times 10^{-3}$ mm Hg exerted no appreciable influence on the percentage content of the ions.

The mass spectroscopic measurements have shown that in probe measurements of the energy spectrum of ions it is necessary to introduce corrections connected with the presence of doubly and triply charged ions. The more accurate values of the average energies are given in Table I.

## 8. DISCUSSION OF RESULTS

Investigations of high velocity plasma streams in stationary vacuum arcs have made it possible to determine with sufficient accuracy such important plasma characteristics as the average velocity of motion, the energy spectrum, and the composition. It turned out that the previously reported anomalous high estimates of ion energies ($3 \times 10^2 - 2 \times 10^3$ eV)[3] were in error. The average energies measured (under identical conditions) by the probe-analyzer method for metals of the first and second group are equal respectively to 5—10 and 20—40 eV, and are close to the voltage drop in the arc (cathode drop). On the other hand, the presence of noticeable amounts of triply charged ions (with ionization potentials 30—40 eV) in the plasma of vacuum arcs is possible if the electron temperature in the ionization region (cathode spots) is comparable with the cathode potential drop. All this allows us to assume that the pressure of the electron gas plays a noticeable role in the acceleration of the ions[17].

It is known that electron gas can perform work and accelerate the ions if $\nabla (n_e k T_e) \neq 0$. If we assume the expansion of the cathode-spot dense plasma in vacuum to be isothermal (owing to the

high thermal conductivity of the plasma in the cathode spot), then the acceleration of the ions should be the result of a large gradient of electron concentration $\nabla n_e$. The field intensity in the case of such (ambipolar) acceleration is given by the expression

$$E = (kT_e / e) \nabla (n_e{}^0 / n_e),\qquad(1)$$

and the potential difference at points with electron concentrations $n_e^0$ and $n_e$ is of the form

$$U_0 - U = 1.5\, e^{-1} w_e \log(n_e{}^0 / n_e),\qquad(2)$$

where $w_e$ —average energy of the electrons in the cathode-spot region, and $n_e^0$ —largest electron concentration. If we assume that $w_e \sim 5-8$ eV and $\log (n_e^0 /n_e) = 3$, then $U_0 - U \approx 20-40$ V.

Inasmuch as the electron concentration decreases in both directions away from the maximum, towards the cathode and from the cathode, a potential "hump" of considerable size should exist in the region of the cathode-spot plasma ($U_0 - U = 20-40$ V; Fig. 6). (An increase of the potential near the cathode was observed for mercury arcs by Lamar and Compton[20]). The high-velocity plasma streams (ions) may be due to the ion acceleration in the region of the potential hump on the anode side. The ions have scattered energy values because they are produced in different sections of the potential hump. The notion of the potential hump explains also a few other peculiarities of vacuum arcs.

Let us estimate the electron temperature and the average plasma concentration in the region of the cathode spots. We define as the cathode-spot region that part of the arc plasma in which the vapor of the cathode metal is ionized and doubly and triply-charged ions are generated. The length of this region, $d_k$ (Fig. 6), will be defined approximately by the relation

$$d_h = v_i t = v_i / \sigma n_e{}^0 v_e,\qquad(3)$$

where $v_i$ —average velocity of motion of the ions or of the neutral particle in the ionization region, $t$ —ionization time, $\sigma$ —average ionization cross
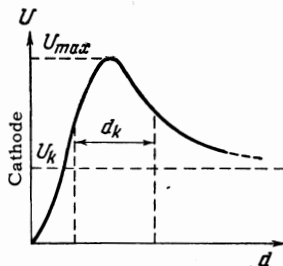


FIG. 6. Assumed potential distribution in the cathode-spot plasma.

section, $n_e^0$ and $v_e$ —electron concentration and velocity averaged over the ionization region. Without commiting a large error, we can put $\sigma = 10^{-17} -10^{-18}$ cm$^2$, $n_e^0 = 10^{18}$ cm$^{-3}$, $v_i = 5 \times 10^5$ cm/sec, and $v_e = 10^8$ cm/sec; we then get $d_k = 5 \times 10^{-4} - 5 \times 10^{-3}$ cm. For mercury arcs, the ionization region apparently coincides with the region of the bright glow, and amounts to $4 \times 10^{-3}$ cm[21]. We shall henceforth put $d_k = 3 \times 10^{-3}$ cm.

The electron temperature of the cathode-spot plasma can be obtained by starting from the experimental data on the population of the plasma with ions of different charge multiplicity (see Table II). Equilibrium concentrations of ions of charge multiplicity $i-1$ and $i$ are connected by the following recurrence relation:

$$N^{+i} = \sigma_{(i-1)\to i}N^{+(i-1)}n_e{}^0 v_e / [\sigma_{i\to(i+1)}n_e{}^0 v_e + 1 / \tau_i],\quad(4)$$

where $N^{+i}$ and $N^{+(i-1)}$ —average concentration of the ions with charge multiplicities $i$ and $i-1$, respectively; $\sigma_{(i-1)\to i}$ and $\sigma_{i\to(i+1)}$ —average cross sections for the production of ions of multiplicities $i-1$ and $i$, respectively; $\tau_i$ —the time spent by the ion of multiplicity $i$ in the region of the cathode spot. Expressing $n_e^0$ in terms of the average values of the pressure $p_e$ (dyne/cm$^2$) and the electron energy $w_e$ (eV), we obtain

$$n_e{}^0 = 7 \cdot 10^{11}\, p_e / w_e.\qquad(5)$$

Substituting (5) in (4) and putting $v_e = 6 \times 10^7\, w_e^{1/2}$, we get

$$\frac{N^{+i}}{N^{+(i-1)}} = \frac{\sigma_{(i-1)\to i}}{\sigma_{i\to(i+1)} + 2.4 \cdot 10^{-20} w_e^{1/2}/\tau_i p_e}.\qquad(6)$$

We further express $\sigma$ in terms of $w_e$, using the empirical formula for the ionization cross section[22]

$$\theta_{(i-1)\to i} = a(\varepsilon - \varepsilon_i)\exp[-b(\varepsilon - \varepsilon_i)],\qquad(7)$$

where $\epsilon_i$ —ionization energy and $\epsilon$ —electron energy. Assuming a Maxwellian energy distribution for the electrons, we obtain for the average ionization cross section

$$\sigma_{(i-1)\to i} = \int_{\varepsilon_i}^{\infty} \theta_{(i-1)\to i}(\varepsilon) j_e(\varepsilon)\, d\varepsilon \,\Big/\, \int_0^{\infty} j_e(\varepsilon)\, d\varepsilon$$

$$= \frac{a \exp(-\varepsilon_i/w_e)}{(b + 1/w_e)^2\, w_e^2} \left[\varepsilon_i + \frac{2}{(1/w_e + b)}\right].\qquad(8)$$

From (7) we determine $a$ and $b$:

$$a = \frac{2.7\theta_i{}^{max}}{\varepsilon^{max} - \varepsilon_i}, \qquad b = \frac{1}{\varepsilon^{max} - \varepsilon_i},\qquad(9)$$

where $\epsilon^{max}$ —electron energy at which the cross section has a maximum. Let us express (9) as a function of $\epsilon_i$. It follows from Thomson's for-

mula[22] that $\theta^{max} = 4 \times 10^{-15}/\epsilon_i^2 [cm^2]$. On the other hand, it has been experimentally established that $\epsilon^{max} = 3.5 \epsilon_i$. By substituting these values in (9) we get

$$a = 4 \cdot 10^{-15}/\epsilon_i^3, \qquad b = 1/2.5 \epsilon_i. \qquad (10)$$

Substituting (10) in (8) we obtain for the ionization cross section the convenient expression

$$\sigma_{(i-1)\to i} = \frac{4 \cdot 10^{-15} \exp(-\epsilon_i/w_e)}{\epsilon_i^2 (1 + w_e/2.5\epsilon_i)^2} \left[ \frac{2}{\epsilon_i/w_e + 0.4} + 1 \right] \cdot (11)$$

Here $\epsilon_i$ and $w_e$ are in electron volts.

From (11) and (6), using the experimental values of $N^{+2}/N^{+1}$ and $N^{+3}/N^{+2}$ (Table II), we can find $w_e$ and the product $\tau_i p_e$. By specifying the time that the ion stays in the ionization region in the form $\tau_i = d_k/d_i$, we obtain $p_e$ and then the electron concentration $n_e^0$ from relation (5). The results of such calculations for aluminum, nickel, and cadmium are listed in Table III.

For more accurate calculations it is necessary to take into account the ionization through excited states (for nickel and cadmium). For metals of the second group the most probable value is $w_e = 6-10$ eV and $n_e^0 \sim 10^{18}$ cm$^{-3}$. For metals of the first group, assuming $\tau_i p_e = 5 \times 10^{-2}$, we get from (6) and (11) $w_e = 3-4$ eV and $n_e^0 = 10^{18}$ cm$^{-3}$. The values of $e(U_0 - U)$, determined from relation (2) with $n_e = 10^{14}$ cm$^{-3}$, are exaggerated compared with the ion energy (Table I), since relation (2) is not sufficiently accurate. Actually, when the plasma expands appreciably the electron temperature decreases, and the process should be described by a polytrope.

The calculated values of the concentration, $\sim 10^{18}$ cm$^{-3}$, are close to the estimates derived from experiments dealing with the effect of the pressure of an external gas on the force of reaction on the cathode[6]. For copper at a gas pressure $6-10$ mm Hg ($N_2$), the anomalous reaction forces disappear, i.e., the conditions in the plasma of the cathode spots change abruptly. This should obviously be observed whenever the external gas concentration $\sim 3-6 \times 10^{17}$ cm$^{-3}$ (after dissociation) becomes commensurate with the concentration in the cathode-spot plasma. The vanishing of the anomalous reaction forces can be attributed to

the sharp decrease in $w_e$ and the lowering of the potential hump.

It is interesting to note that in the same pressure range (from 10 mm Hg and above), the backward motion of the cathode spot changes into a forward motion[10]. It is natural to assume that the backward motion is also connected with the existence of the potential hump. The magnetic field in the region of the cathode spots is somewhat weaker in the forward spot direction. Therefore the plasma has a tendency to flow out in larger quantities in this direction, and this produces a reaction on the region of the cathode spot, causing the latter to move backwards. Thus, the notion of the potential hump makes it possible to explain the high speed plasma streams and the backward motion from a unified point of view. It also becomes possible to explain the transport of energy to the cathode. The average kinetic energy of the ions accelerated in the region of the potential hump and the cathode drop reaches $\sim 50$ eV, even $\sim 65$ eV if the potential energy is taken into account. The ion flux to the cathode is approximately equal to the flux from the cathode, the latter amounts (in terms of the number of particles) to $5-10\%$ of the total energy released in the cathode-spot plasma (the plasma is obviously heated by the electrons, which are accelerated in the region of the cathode potential drop). Our experiments with brass have shown that the cathode actually receives $25-30\%$ of the energy.

The "two-thirds" law was used in many papers[20,21] to estimate the length of the cathode potential drop region, assuming zero ion velocity. The presence of a potential hump and high initial ion energies makes such calculations doubtful. The length of the cathode-drop region can become appreciable ($\sim 10^{-3}$ cm), and the cold-emission mechanism is no longer adequate. It is advantageous to turn again to the mechanism of thermoelectric emission.

Tentative calculations show that the experimentally observed electron emission densities ($\sim 10^6$ A/cm) and evaporation densities ($\sim 10^{24}$ particles/cm$^2$ sec) can be attained at a cathode temperature $\sim 5 \times 10^3$ deg K. The possibility of existence of superheated states of metals for a short time ($\sim 10^{-6}-10^{-7}$ sec) was experimentally proved in explosions of wires[23].

In conclusion the authors thank L. I. Chibanova for help with the work.

### Table III

| Metal | $w_e$, eV | $10^3\tau_i p_e$, g/sec-cm | $10^9\tau_i$, sec | $10^{-6}p_e$, g/sec$^2$-cm | $10^{-17}n_e^0$, cm$^{-3}$ | $U_0-U$, V |
|---|---|---|---|---|---|---|
| N i | 27 | 0,9 | 3,5 | 2,6 | 0,7 | 130 |
| Ni | (10)* | (4,6) | (3,5) | (13) | (9) | (48) |
| Al | 6,5 | 5,2 | 2 | 26 | 34 | 31 |
| Cd | 3,4 | 5 | 10 | 5 | 10 | 17 |

*Proposed value.

[1] R. Tanberg, Phys. Rev. 35, 1080 (1930).

[2] R. Tanberg and W. Berkey, Phys. Rev. 38, 296 (1931).

[3] E. Kobel, Phys. Rev. 36, 1636 (1930).

[4] L. Tonks, Phys. Rev. 50, 226 (1936) and 54, 634 (1938).

[5] Easton, Lucas, and Creedy, Trans. AIEE 53, 1454 (1934).

[6] R. Robertson, Phys. Rev. 53, 578 (1938).

[7] K. Compton, Phys. Rev. 36, 706 (1930); Proc. Nat. Acad. Sci. 18, 705 (1932).

[8] L. Tonks, Phys. Rev. 46, 278 (1934).

[9] C. G. Smith, Phys. Rev. 62, 48 (1942) and 84, 1075 (1951).

[10] R. M. St. John and I. G. Winans, Phys. Rev. 94, 1097 (1954) and 98, 1664 (1955).

[11] G. A. Farrall and G. H. Reiling, J. Appl. Phys. 32, 1528 (1961).

[12] I. G. Kesaev and L. A. Levshenkova, ZhTF v. 30, 815 (1960), Soviet Phys. Tech. Phys. 5, 768 (1961); I. G. Kesaev, ZhTF 29, 1462 (1959) and 30, 674 (1960), Soviet Phys. Tech. Phys. 4, 1351 (1960). and 5, 635 (1960).

[13] J. D. Cobine and C. J. Gallagher, Phys. Rev. 74, 1524 (1948); J. Somerville and W. Blevin, Phys. Rev. 76, 982 (1949).

[14] K. D. Frome, Proc. Phys. Soc. London 60, 424 (1948); 62, 805 (1949); 63, 377 (1950); J. Appl. Phys. 24, 91 (1953).

[15] N. M. Zykova, Izv. AN SSSR ser. fiz. 26, 872 (1962), Columbia Tech. Transl. p. 873; H. S. Dunkerley and D. L. Schoefer, J. Appl. Phys. 26, 1384 (1955).

[16] T. H. Lee, J. Appl. Phys. 28, 920 (1957); 29, 734 (1958); 30, 166 (1959). J. H. Lee and A. Greenwood, J. Appl. Phys. 32, 917 and 2061 (1961).

[17] A. A. Plyutto, JETP 39, 1589 (1960), Soviet Phys. JETP 12, 1106 (1961).

[18] W. Berkoy and R. Mason, Phys. Rev. 38, 943 (1931).

[19] A. Dempster, Rev. Sci. Instr. 7, 46 (1936).

[20] E. Lamar and K. Compton, Phys. Rev. 37, 1069 (1931).

[21] C. G. Smith, Phys. Rev. 69, 96 (1946).

[22] V. L. Granovskiĭ, Elektricheskiĭ tok v gazakh (Electric Current in Gases), Gostekhizdat, 1952.

[23] Kvartskhava, Plyutto, Chernov, and Bondarenko, JETP 30, 42 (1956), Soviet Phys. JETP 3, 40 (1956).